Heterogeneous and Nonisothermal Mixing of a Lateral Jet with a Swirling Crossflow

Yei-Chin Chao*
National Cheng Kung University, Tainan, Taiwan 70101, Republic of China
and
Wu-Chi Ho†
Industrial Technology Research Institute, Hsinchu, Taiwan 31015, Republic of China

The heterogeneous and nonisothermal mixing of a lateral jet discharging into a confined swirling or nonswirling crossflow is studied numerically. The grid effect and the error due to numerical diffusion and skewness are first assessed, and the results are compared with the existing experimental and numerical data base. The complicated three-dimensional swirling mixing phenomena are delineated and the jet-coupling character of the jet in the swirling crossflow is identified. The density effect, caused by the heterogeneous and nonisothermal mixing on the jet trajectory, the decay of the jet strength, and the jet spread and mixing for both swirling and nonswirling cases are also analyzed.

Nomenclature

A = cross-sectional area
C = mass fraction
D = test-section diameter
d = jet nozzle diameter
J = jet-to-crossflow momentum ratio
K = turbulent kinetic energy
L = tube length
M = jet-to-crossflow mass flux ratio
R = jet-to-crossflow velocity ratio
R_e = Reynolds number
S = source term
T = temperature
u, v, w = velocity components
V = total velocity
X = axial coordinate
$\bar{X}, r, \theta$ = axial, radial, and azimuthal coordinates, respectively
Γ = exchange coefficient
ε = dissipation rate of turbulent kinetic energy
η = diffusion parameter
μ_e = effective viscosity
ρ = density
σ = turbulent Prandtl/Schmidt number
Φ = swirl vane angle
ϕ = dependent variable

Subscripts
C = mass fraction
D = diffusion area
h = swirler hub
in = tube inlet
j = along the velocity or temperature trajectory of jet
mr = maximal value at a certain radius
o = jet inlet
rms = root mean square
T = temperature
ϕ = for dependent variable

Superscripts
$*$ = nondimensional value
$'$ = fluctuation component

Presented as Paper 88-3190 at the AIAA/ASME/SAE/ASEE 24th Joint Propulsion Conference, Boston, MA, July 11–13, 1988; received March 20, 1990; revision received July 19, 1990; accepted for publication July 20, 1990.

*Associate Professor, Institute of Aeronautics and Astronautics. Member AIAA.
†Research Scientist, Energy and Resources Laboratories.

Introduction

THE flow of jets discharging into a larger cross-stream commonly occurs in effluent dispersion operations and in industrial processes where streams are mixed for dilution, heat transfer, or chemical reaction. In gas turbine application, jet injection plays an important role in the enhancement of combustor performance both in the primary and dilution zones. Because of its practical importance, various experimental, computational and theoretical investigations have been performed on the flow phenomena of jet injection and mixing, and a fairly thorough review has been given by Schetz[1] and, more recently, by Sherif and Pletcher.[2] Most of the published works were concentrated on homogeneous and isothermal mixing of the lateral jets with the nonswirling crossflow, for example, the works of Andreopoulos,[3] Atkinson et al.,[4] and Patankar et al.[5] On the other hand, heat transfer and density effects involved in the nonisothermal mixing of the lateral jet and the crossflow were studied by Andreopoulos,[6] Kamotani and Greber,[7] Jones and McGuirk,[8] Holdeman and Srinivasan,[9] and Sherif and Pletcher[10] for nonswirling cases. In the modern gas turbine combustor, swirl is extensively used to enhance the combustion. Therefore, the topic of jet injection into confined swirling crossflow is of great interest in the combustor research community recently. Lilley[11] and McMurry et al.[12] presented studies of isothermal and homogeneous mixing of the lateral jets and the swirling crossflow. One of the major concerns in the gas turbine combustor design is the temprature pattern factor at the combustor exit. The mixing of the lateral dilution jets and the swirling burnt cross stream is the key factor to a well-defined pattern factor. Thus, the temperature and density effects on the mixing of the jets in the swirling crossflow are important issues. Only very few recent articles have concentrated on this problem. So and Ahmed[13] studied the characteristics of a helium jet injected into a coaxial swirling airflow experimentally. Chao and Ho[14] numerically investigated the nonisothermal mixing of the lateral jet with the swirling crossflow. Ho[15] studied the mixing with density difference between the lateral jet and swirling crossflow. These papers presented the primary studies of the

mixing characteristics in the swirling crossflow. However, the detailed three-dimensional mixing mechanism is still not fully discussed.

The present work numerically investigates the three-dimensional mixing between the lateral jets and the swirling crossflow, with temperature and species difference. The influencing parameters are correlated and reduced, and the dominant factors are also discussed and identified. Furthermore, the numerical error, which occurs in the computation of this complex flow, is discussed.

Analysis

For steady flow, the turbulent Reynolds equations for mass, momentum, turbulent kinetic energy, dissipation rate, thermal energy (temperature), and species (mass fraction) in three-dimensional cylindrical polar coordinates can be written in the common conservative form.

$$\frac{\partial}{\partial x}(\rho u\phi) + \frac{1}{r}\frac{\partial}{\partial r}(\rho r v\phi) + \frac{1}{r}\frac{\partial}{\partial \theta}(\rho w\phi) = \frac{\partial}{\partial x}\left(\Gamma_\phi \frac{\partial \phi}{\partial x}\right) + \frac{1}{r}\frac{\partial}{\partial r}\left(r\Gamma_\phi \frac{\partial \phi}{\partial r}\right) + \frac{1}{r}\frac{\partial}{\partial \theta}\left(\Gamma_\phi \frac{\partial \phi}{r\partial \theta}\right) + S_\phi \quad (1)$$

For the continuity equation, $\phi = 1$. The standard $K-\varepsilon$ two-equation model[16] was implicitly used here to close the solution. Γ_ϕ is the appropriate effective exchange coefficients for the turbulent flow and S_ϕ is the source term. Definitions of Γ_ϕ and S_ϕ are referred to in Ref. 17. The differencing technique employed was the hybrid scheme for convective terms with central differencing for all other terms. The resulting discrete equations were solved iteratively by the SIMPLEC[18] procedure. When the residuals in mass, momentum, and kinetic energy were reduced below 4×10^{-3}, the computation was terminated. For the flow presently considered, the temperature difference ($\Delta T < 150$ K) and density ratio ($\rho/\rho_{air} < 2$) between the lateral jet and the cross stream were sufficiently small that density fluctuations were considered negligible.[8] In other words, the constant density model was applied to solve the Reynolds/Favre averaged equations. Both temperature and mass fraction were considered to be passive scalars, and the T and C equations contain no source terms. The exchange coefficients for temperature and mass fraction equations were approximated by the appropriate effective viscosity and the turbulent Prandtl/Schmidt number ($\sigma_{t,T}$ and $\sigma_{t,C}$) as

$$\overline{\rho u'\phi'} = -\frac{\mu_e}{\sigma_{t,\phi}}\frac{\partial \phi}{\partial x} \quad (2)$$

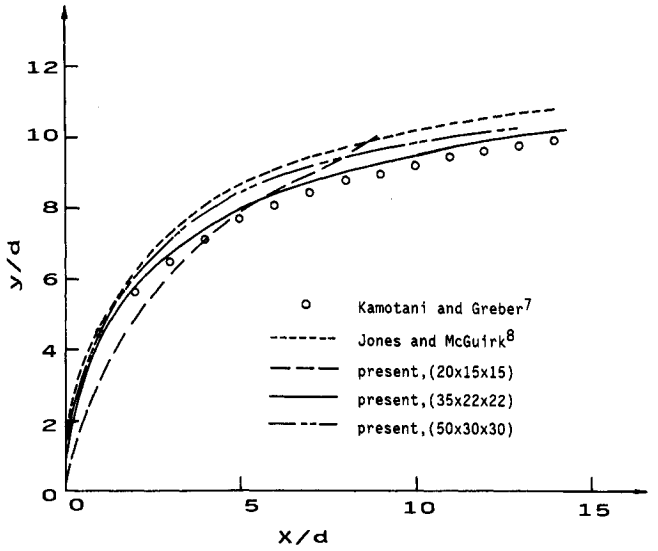

Fig. 1 Predicted and measured jet temperature trajectories with momentum ratio J = 32.

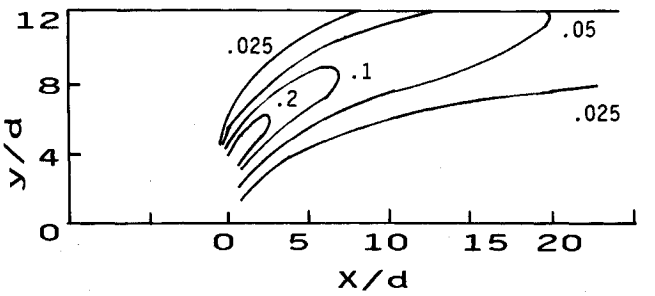

a) Contours measured by Kamotani and Greber[7]

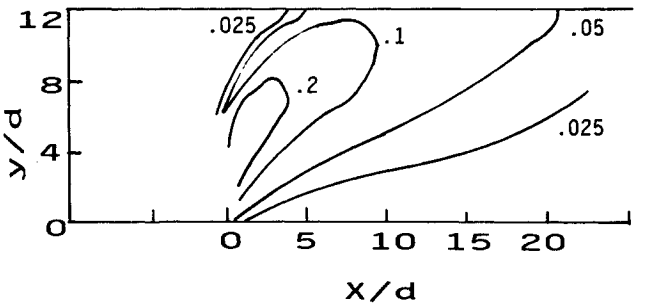

b) Contours computed by Jones and McGuirk[8]

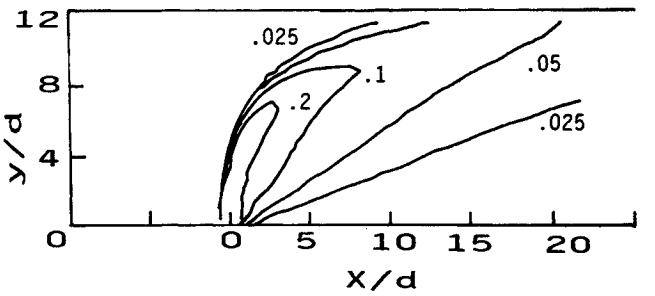

c) Predicted contours on the 50 × 30 × 30 grid system

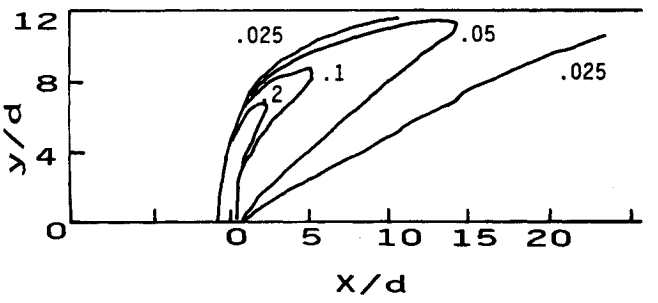

d) Predicted contours on the 35 × 22 × 22 grid system

Fig. 2 Measured and predicted nondimensionalized temperature contours on the symmetric plane.

In general, the value of $\sigma_{t,\phi}$ is of the order of 1 and $\sigma_{t,\phi}$ mainly affects the diffusivity of the scalar field. In order to assess the effect of the turbulent Prandtl/Schmidt number, a number of computer runs were carried out for $\sigma_{t,\phi}$ changing from 0.5 to 0.9. From the computed results of temperature contour pattern, no significant changes were found. Therefore, the value of $\sigma_{t,0\phi}$ was set at 0.9, as suggested by Jones and McGuirk,[8] in the latter computations. The error due to the grid system with respect to the scheme in the prediction of complicated turbulent flow is important. In order to look into the effect of grid on the prediction, the numerical experiments were performed on a hierarchy of grid systems. It was found[15] that grid independence became a formidable task

in terms of the computational expense. The grids 43 × 26 × 32 and 60 × 26 × 17 appear to be adequate[15] in terms of accuracy for the computations of swirling and nonswirling cases, respectively.

Computer runs were made to examine the capability of the computer program on the prediction of nonisothermal mixing. The test problem was a heated circular jet injected into a rectangular crossflow. The temperature difference between the jet and crossflow was 167 K and the jet-to-crossflow momentum ratio J was 32. The flow geometry was used by Kamotani and Greber[7] for experiment and by Jones and McGuirk[8] for computation; the calculated results are compared in Figs. 1 and 2. Because the 20 × 15 × 15 grid used by Jones and McGuirk[8] was too coarse, the false diffusion and the skewness error caused by the hybrid scheme in the curvilinear region of the deflected jet became significant. Satisfactory prediction, based on the comparison of the present results of the jet temperature trajectory (Fig. 1) and temperature contour (Figs. 2) with the measurements of Ref. 7 was obtained by using the moderate grid. When the fine grid was employed and, hence, the false diffusion and the skewness error were reduced, the computation underestimated the jet temperature trajectory and the mixing between the jet and crossflow. It was observed,[19] by analyzing the distributions of the relative magnitudes of the false numerical diffusion error and the convection and diffusion terms, that the false diffusion became important only around the jet flow and grid refinement had positive improvement on the false diffusion error. This revealed that the deficiencies of the $K-\varepsilon$ turbulence model became significant as the numerical error was reduced.

The computational geometry is shown in Figs. 3. The incoming airstream may possess a swirl velocity component by passing through the swirler. The carbon dioxide, or air jet, which may be heated or unheated, is injected at one test-section diameter downstream of the crossflow inlet. The dimensions are $D = 0.15$ m, $d = 0.1\,D$, $L = 50\,d$, $D_h = 0.25\,D$, and R_{eD} eq 1.51×10^5. For swirling crossflow cases, the swirl vane angle $\Phi = 45$ and 70 deg.

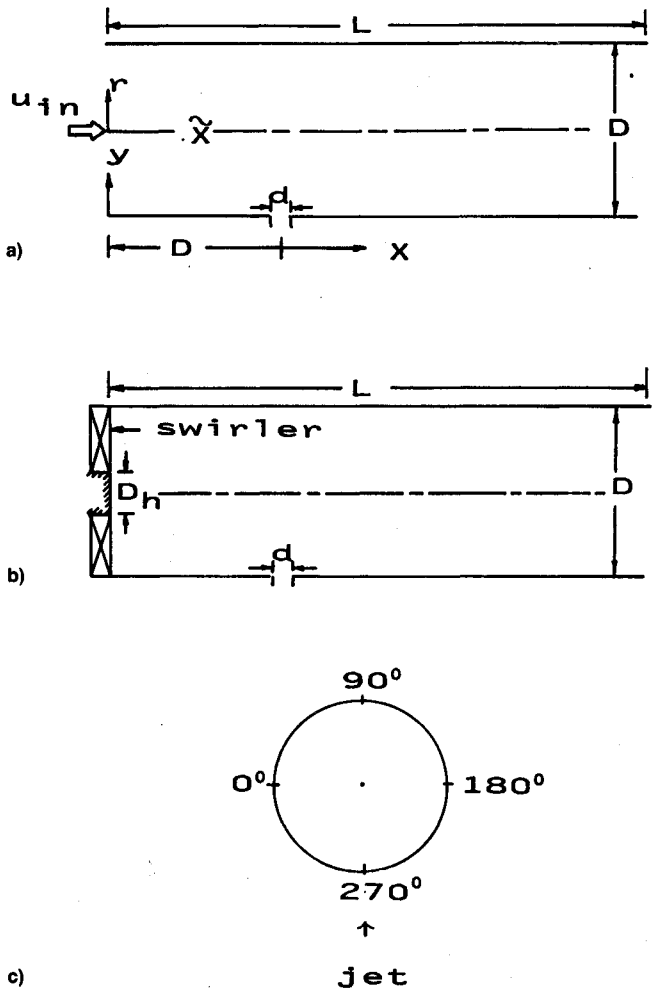

Fig. 3 Computational configurations: a) nonswirling cases; b) swirling cases; c) definition of angle.

Results and Discussion

Cases of Nonswirling Crossflow

The basic homogeneous mixing phenomena of the jet in the nonswirling crossflow have been discussed in length in a previous paper by Chao and Ho,[14] and the findings of the basic flow phenomena are summarized here. As the jet is injected into the crossflow, a pair of vortices, which are induced by the interaction of the crossflow with the jet column, can be observed in the near field to attach to the lee side of the jet column. The jet cross section is then gradually distorted into the kidney shape due to the presence and growth of the vortices, which become slender as the jet column is deflected in the downstream. When the jet moves farther downstream, the vortices expand over the whole jet cross section. Thus, the jet fluid is pulled into its own wake and the jet loses its identity in the velocity contour plot. Therefore, the induced vortices become dominant in the downstream region. From the point of view of turbulence, the experimental results of Andreopoulos and Rodi[20] indicated that strong correlation was found between the mean velocity gradient $\partial u/\partial r$ and the turbulent kinetic energy. The peak positions of the $\partial u/\partial r$ profile corresponded to the maximal positions of the normal and shear stresses; these peak positions were observed[14] to lie on the lee side of the jet. Therefore, the transition of the jet in the crossflow and the generation and growth of the vortices are closely related to the velocity gradient $\partial u/\partial r$ induced by turbulence.

In order to reveal the density effect on the mixing characteristics, the jets with different species or temperature injected into the nonswirling cross airstream were first investigated. The conditions of the jets are listed in Table 1.

Jet trajectory is one of the most important characteristics in the studies of jet-in-crossflow problems. The velocity trajectories of the A, B, and C jets, which have the same momentum ratio, are shown in Fig. 4. The velocity trajectory is defined to be the locus of the local maximum total velocity. The trajectories for the A, B, and C jets are found to be nearly identical in Fig. 4. From the experiments conducted by Kamotani and Greber,[7] the heated jet motion is observed to be inertially dominated, with buoyancy playing only a minor role. Therefore, the trajectory depends mainly on the jet-to-crossflow momentum ratio. Generally, the present results are consistent with the experimental findings.[7]

Along each velocity trajectory, the decay process of the jet velocity with respect to the jet injection velocity for the A, D, and E jets with the same R ratio are given in Fig. 5. It is apparent that the decay processes for these identical R-ratio jets are similar. There exists a similarity rule for the decay of the jet velocity along the jet velocity trajectory, and the decay process is dominated by the jet-to-crossflow velocity ratio R.

Table 1 The jet conditions

Jet	Species	ΔT	$\rho_{jet}/\rho_{air}^{cross}$	R[a]	M[b]	J[c]
A	air	0	1	4	4	16
B	air	150	0.664	4.9	3.26	16
C	Carbon dioxide	0	1.51	3.26	4.92	16
D	air	50	0.855	4	3.42	13.7
E	air	150	0.664	4	2.66	10.6

[a]R: Jet-to crossflow velocity ratio.
[b]M: Jet-to crossflow mass flux ratio.
[c]J: Jet-to crossflow momentum ratio.

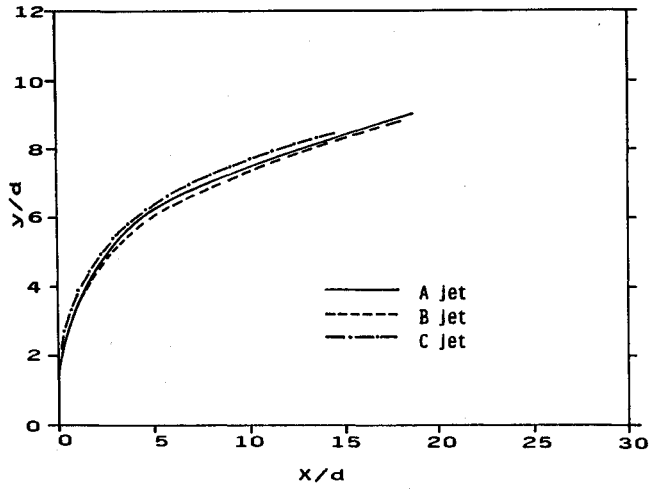

Fig. 4 Effect of the jet-to-crossflow momentum ratio on the jet velocity trajectory.

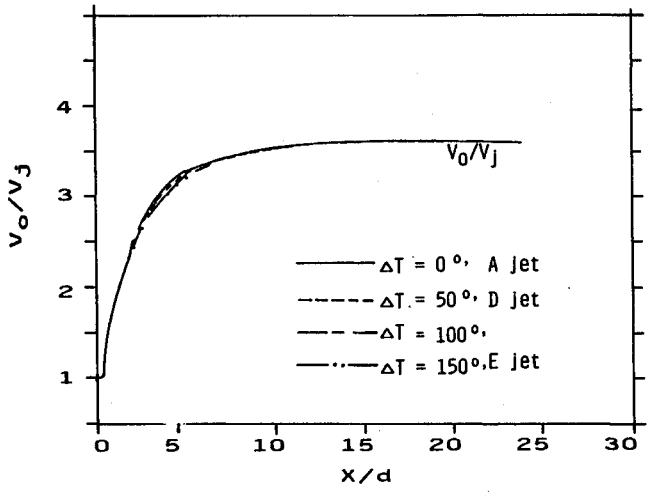

Fig. 5 Temperature effect on the decay processes of the jet velocity along the trajectory.

The property of jet expansion can be described by a diffusion parameter η, which is defined as

$$\eta = A_D/A \tag{3}$$

where A denotes the area of the tube section and A_D is the area of influence. A_D is defined to be the area enclosed by the nondimensionalized passive scalar contours of certain values in the axial locations. For example, for the nonisothermal case, A_D was chosen to be the area enclosed by the nondimensionalized temperature contour of value 0.03 in the axial locations. The value was chosen because the nondimensionalized temperature approached 0.0384 for the complete mixing condition. The effect of the contour value for A_D was tested and discussed by Ho.[15] This diffusion parameter is useful for describing the overall mixing characteristics, especially for the cases of mixing with density difference. For each η curve given in Fig. 6, in the region of $X/d < 4$, η increases very rapidly because the strong vortex motion enhances the jet spreading. In the downstream region, the η curves appear linear. Although the A, B, and C jets have the same momentum ratio, their η curves are apparently different. The jets with higher mass ratio have faster growth rate of η. In other words, the heavier jets spread faster than the lighter jets. Considering the B and D jets, these two jets possess almost the same mass ratio, whereas the momentum ratio of the former is larger than that of the latter. Thus, the B jet

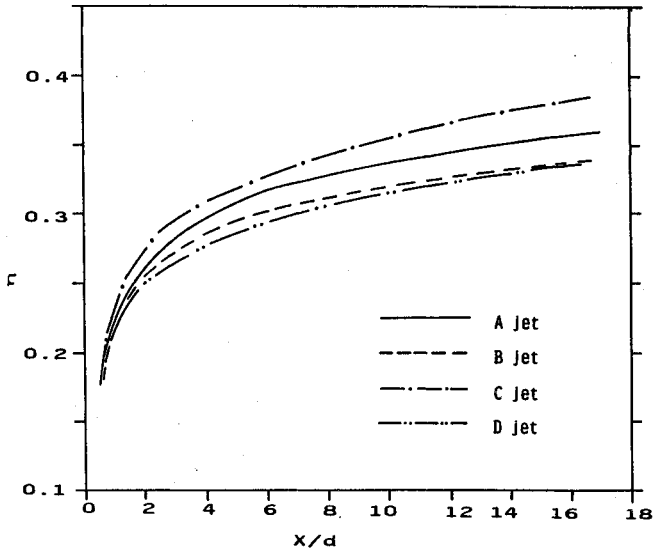

Fig. 6 Development processes of the diffusion parameter of the A, B, C, and D jets.

spreads faster than the D jet in the near-field region because of its stronger vortex motion. However, their η curves will eventually merge together in the downstream region. Therefore, the development of the diffusion parameter in the downstream region is mainly dependent on the mass ratio.

Cases of Swirling Crossflow

The transition of the jet in the swirling crossflow is different from that in the nonswirling case. The addition of the tangential velocity component and the swirl-induced radial pressure gradient will completely alter the jet trajectory and mixing characteristics. In general, the jet behavior in the swirling crossflow is complicated and three dimensional. The trajectories of the jet in the swirling and nonswirling crossflow cases are compared in Fig. 7. It shows completely different phenomena of jet deflection and penetration into the main stream. As shown in Fig. 7, the deformation process of the jet in the swirling crossflow can be divided into three stages. First, after being injected, the jet is slightly deflected in the tangential direction while it penetrates into the crossflow. The second stage can be defined by the curvilinear region of the jet deflection around the peak penetration. As the jet penetrates into the crossflow, the jet is initially spiraling with a small spiral angle, and the spiral angle becomes larger in the second stage so that the deflection of the jet as shown in Fig. 7

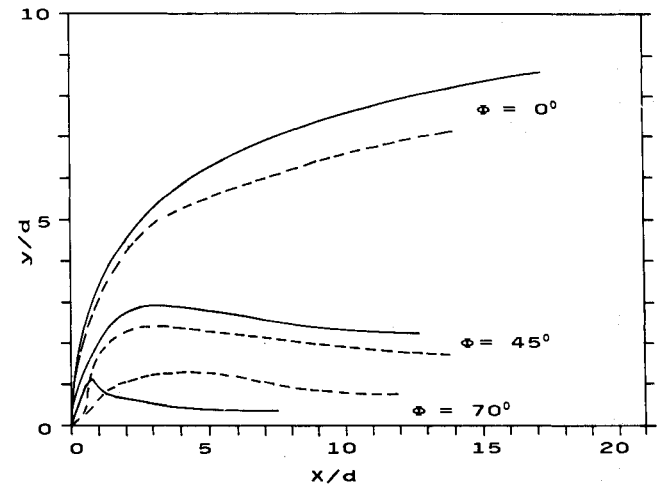

Fig. 7 Effect of the swirl on the jet trajectories, R = 4: —velocity trajectory; – – –scalar trajectory.

becomes significant. In the final stage, the jet moves radially toward the wall as it spirals after the peak penetration. This can be explained from the viewpoint of the hydrodynamic stability.[21] This outward motion of the jet is induced by the unbalanced centrifugal force near the jet. Considering a fluid element in the swirling flow, when in equilibrium, the centrifugal force is balanced by the local pressure force exerted by the surrounding fluids. If the centrifugal force is larger than that of the fluid situated at a larger radial location, the jet will move toward the tube wall due to an outward pressure gradient. This instability can be described by a criterion that the jet will move outward when the term $(d/dr)\ (r^2w^2) < 0$ in the region around the jet. From the tangential velocity profile of the present flow,[15] it was found that the jet has a larger tangential velocity component than the neighboring fluid located at a larger radial position. Consequently, in the initial stage, the jet penetrates into the swirling flow as a result of the prevailing inward momentum. However, the jet fluid is then displaced radially outward in the following stage due to the outward pressure gradient as the jet strength becomes weaker after the peak penetration. Therefore, swirl reduces the jet penetration. It is partly due to the additional swirl velocity component that reduces the true local jet-to-crossflow velocity ratio. In other words, the radial pressure gradiant induced by the swirl component prevents the jet from penetration. In addition, the excess turbulent mixing of the jet with the swirling crossflow further decays the jet.[14] In order to study the spread of the jet fluid in the swirling crossflow, the passive scalar field was calculated. In the cases of homogeneous or isothermal mixing, the passive scalar field was computed by artificially adding a negligible amount of scalar (temperature or density) into the jet. The jet penetration determined from the passive scalar trajectory, which was defined as the locus of the local points of the maximum scalar value, is also shown in Fig. 7 for comparison. Because the induced vortices behind the jet gradually expand over the jet cross section, the jet fluid is pulled into its own wake. Thus, the scalar trajectory falls below the velocity trajectory. For stronger swirling crossflow, $\Phi = 70$ deg, the resultant jet (total) velocity trajectory is so obscure as compared with the scalar (temperature) trajectory that the use of the maximum total velocity to trace the jet behavior may be misleading, especially in the postpeak region where the jet is smeared and loses its identity in the strong swirling crossflow.

In the sequential plots of Figs. 8, the jet spreading on different θ planes can be observed by the constant scalar contours in the $\Phi = 45$ deg swirling crossflow. Here, the scalar is denoted by the mass fraction of the species with respect to the jet injection. It is evident that the jet moves along a spiral path. Because of the hydrodynamic instability[21] of the jet in the swirling crossflow, the jet can hardly diffuse radially into the central region at $X/d < 15$, such that the axial and tangential diffusion of the jet are prevailing in this region. Another interesting feature of the jet spread is found in Fig. 8c. On the $\theta = 350$ deg plane, the tail of the front jet flow is seen to merge with the front portion of the rear jet column due to the fact that the spiraling of the front jet is slowed down as the jet strength is decayed in the downstream and the rear jet merges with the front jet and becomes part of the front jet, which can be noted in Figs. 8d and 8e in the following stage of the mixing process. This phenomenon is identified and is named jet coupling. It is a unique character of the jet in the swirling crossflow that does not exist in the nonswirling case. After the jet coupling, in the downstream region of $X/d > 15$, the merged jet starts to expand radially very rapidly.

Strong spreading also occurs in the tangential direction, as seen in the sequential crosssectional views at several axial locations in Figs. 9. In the initial stage of the jet mixing process, the jet spreading is confined in the outer layer as the jet spirals. The jet annulus closes near $X/d = 12$, approximately the location of jet coupling. Farther downstream, the rear convects into the front jet to form an annulus and starts to

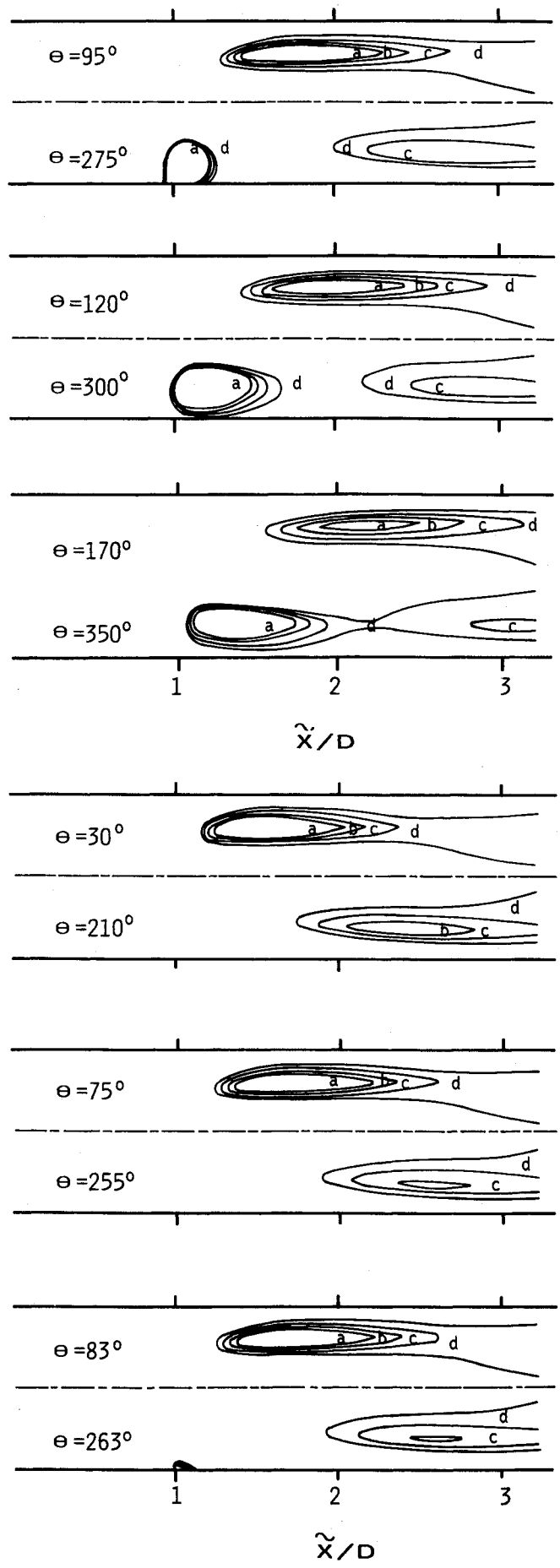

Fig. 8 Constant mass fraction contours of the jet spread on sequential constant planes: a—0.1; b—0.08; c—0.06; d—0.04.

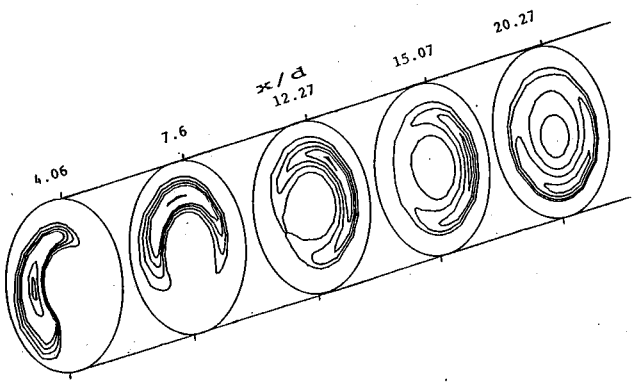

a)

Fig. 9a Constant mass fraction contours of the jet spread as viewed on sequential cross-sectional planes at different axial locations.

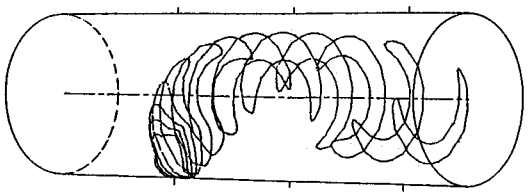

b)

Fig. 9b Three-dimensional view of the jet evolution, as denoted by mass fraction $C = 0.06$, in the swirling crossflow.

diffuse radially into the tube center while preserving the annular shape. Moreover, the contours tend to be axisymmetric. This radial diffusion process can reduce the distortion of the temperature profile at a given radius around the combustor circumference. It is a very important mixing process for the mixing of the combustor dilution jets with the swirling crossflow. From the experimental measurements by Ahmed and So[22] of axial velocity contours on two constant X planes, it can be found that the shape of the influence region of the jet appears to be an annulus. Their measurements provided a crude evidence of the existence of the jet coupling. By employing a three-dimensional graphic technique, the jet evolution, as denoted by the contour of mass fraction $C = 0.06$, in the swirling crossflow is described in Fig. 9b.

Figure 10 presents the temperature, species, and swirling effects on the scalar (temperature) trajectory as compared with the unheated air jet. For the cases of nonconstant density mixing, the density effect needs to be included in the hydrodynamic instability analysis, i.e., the flow will be unstable if $(d/dr)\ (\rho r^2 w^2) < 0$.[21] Since the heated jet has the smallest density as compared with the unheated air and CO_2 jets, the heated jet is the most stable in the swirling crossflow among these three cases. For cases of injection into the crossflow of the same swirl strength, the jets will approach the same depth in the far-field region $X/d > 10$, although the unheated and the CO_2 jets penetrate deeper initially. The CO_2 with larger density, thus higher jet-to-crossflow momentum ratio, has deeper penetration. This phenomenon is similar to the nonswirling cases. The effect of jet injection on the turbulence is given in Fig. 11a where the distributions of axial normal stresses of the swirling flow with and without jet injection on the $\theta = 150$ and 330 deg plane are compared. Because there is a strong shear force exerted on the jet, the turbulence is enhanced locally around the jet. This phenomenon can be observed in Fig. 11a where the jet locates around $\tilde{X}/D = 2.5$, $r/d = 2.1$, and $\theta = 330$ deg. Additionally, the normal stress near the tube center is significantly enhanced by the jet. This indicates that the strength of the central core is intensified.

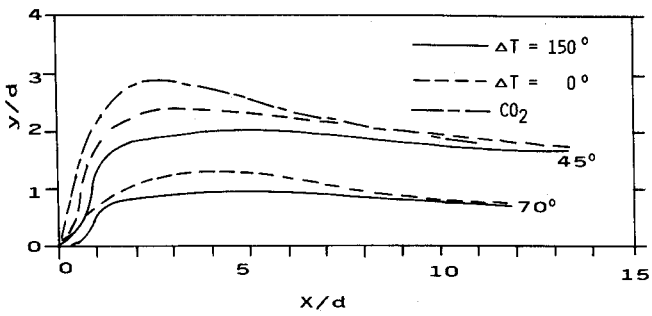

Fig. 10 Comparison of the temperature, species, and swirling effects on the scalar trajectories of the jet in the swirling crossflow, $R = 4$.

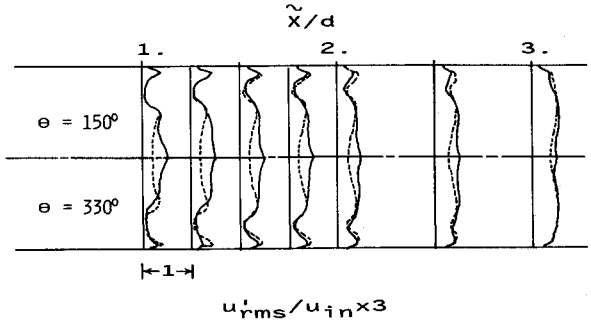

Fig. 11a Effect of the jet injection on the turbulent characteristics of the swirling crossflow: ---without jet injection; —with jet injection.

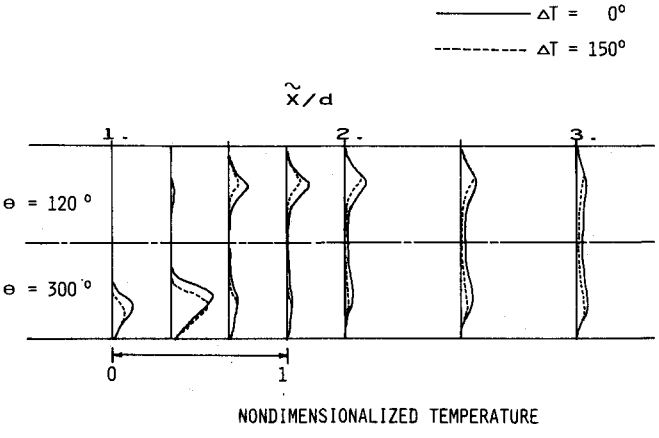

Fig. 11b Temperature effect on the nondimensionalized temperature distribution in the 45-deg swirling crossflow.

This can also be observed by comparing the targential velocity profile around the centerline of the cases with and without jet injection.[15] Therefore, the jet injection not only enhances the turbulence of the swirling flow near the spiraling jet but also around the central vortex core. The temperature effect on the temperature distribution for the swirling cases is shown in Fig. 11b. Since the isothermal jet with larger density can penetrate deeper and generate higher turbulence level around the jet and near the tube center,[14] more uniform profiles are noted, as expected, for the isothermal case in the figure downstream. The jet coupling process was observed in the nonisothermal case. However, the jet coupling occurs farther downstream as compared with the isothermal case. This can vaguely be seen in Fig. 11a at $\tilde{X}/D = 3$. For the isothermal case, the temperature has diffused radially to the central region producing a more uniform temperature distribution, whereas for the nonisothermal case, the jet with higher temperature is still confined in the outer layer. Thus, the temperature effect reduces the jet mixing with the swirling crossflow and delays the jet coupling. The species (density) effect on the heterogeneous mixing is observed in Fig. 12 through

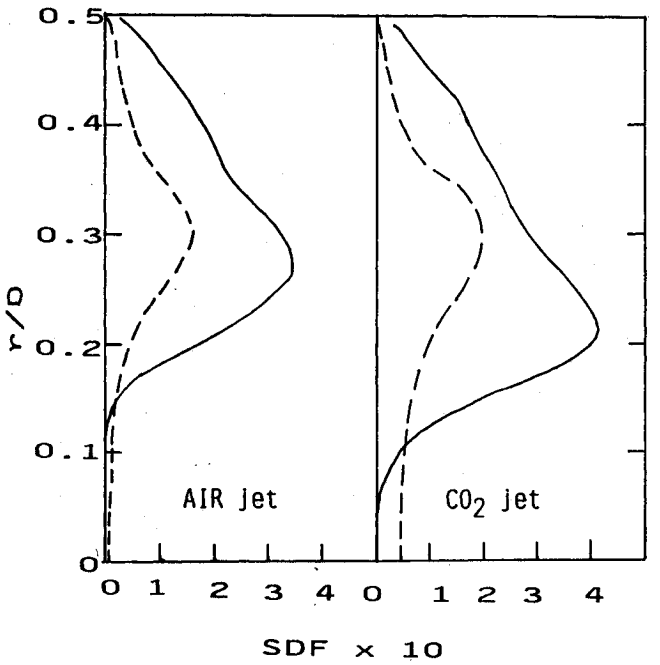

Fig. 12 SDF profiles for the heterogeneous mixing in the 45-deg swirling crossflow: —X/d = 2.3; – – –X/d = 8.7.

a mixing parameter species distribution factor (SDF), which is defined as

$$\text{SDF} = \frac{C_{mr} - C_{in}}{C_0 - C_{in}} \tag{4}$$

From the SDF profiles, the density effect on the penetration depth, the radial shift of the peak due to instability in the downstream region, and the radial diffusion of the jet are clearly evident. As discussed earlier, the heavier jet, the CO_2 jet, has deeper penetration and is more unstable in the swirling crossflow. Therefore, the CO_2 jet has faster radial diffusion and results in wider spread and better mixing with the swirling crossflow.

Conclusions

The heterogeneous and nonisothermal mixing found in the flow of a lateral jet injected into a confined swirling and nonswirling crossflow is studied numerically. The computational results of the test problem are first compared with the experimental data and the existing numerical data base, the grid effect as well as the error due to numerical diffusion and skewness are also assessed. The present emphasis is placed on the complicated three-dimensional swirling mixing phenomena as well as the density effect, caused by heterogeneous and nonisothermal mixing, on the jet trajectories and the jet spread and mixing.

The jet trajectory is found to be dependent mainly on the inlet jet-to-crossflow momentum ratio for nonswirling cases. However, in the swirling cases, the trajectory is dependent not only on the momentum ratio but also on the swirling hydrodynamic instability and the density effects of the heterogeneous and nonisothermal mixing in the postpeak penetration region. The heavier jets, the jets with higher density ratio, spread faster than the lighter ones for both swirling and nonswirling cases. Because of the effect of the swirling, the jet spreading is confined in the outer layer such that radial diffusion into the central vortex core is prohibited in the near-field region. The prevailing of the axial and tangential diffusion generates the jet coupling phenomenon as the jet is spiraling in the swirling crossflow. After the jet coupling, the jet diffuses rapidly to form an annulus and starts to diffuse radially into the central core.

References

[1]Schetz, J. A., "Progress in Astronautics and Aeronautics," *Jet Injection and Mixing in Turbulent Flow*, Vol. 68, AIAA, New York, 1980.

[2]Sherif, S. A., and Pletcher, R. H., "Jet-Wake Thermal Characteristics of Heated Turbulent Jets in Cross Flow," AIAA Paper 88-3725, July 1988.

[3]Andreopoulos, J., "Measurements in Jet-Pipe Flow Issuing Perpendicularly into a Cross Stream," *Journal of Fluids Engineering*, Vol. 104, March 1982, pp. 493–499.

[4]Atkinson, K. N., Khan, Z., and Whitelaw, J. H., "Experimental Investigation of Opposed Jets Discharging Normally into a Cross-stream," *Journal of Fluid Mechanics*, Vol. 115, February 1982, pp. 493–504.

[5]Patankar, S. V., Basu, D. K., and Alpay, S. A., "Predictions of the Three Dimensional Velocity Field of a Deflected Turbulent Jet," *Journal of Fluids Engineering*, Vol. 99, No. 4, 1977, pp. 758–762.

[6]Andreopoulos, J., "Heat Transfer Measurements in a Heated Jet-Pipe Flow Issuing Into a Cold Cross Stream," *Physics of Fluids*, Vol. 26, No. 11, 1983, pp. 3201–3210.

[7]Kamotani, Y., and Greber, I., "Experiments on Confined Turbulent Jets in Cross-flow," NASA CR-2392, March 1974.

[8]Jones, W. P., and McGuirk, J. J., "Computation of a Round Turbulent Jet Injection into a Confined Crossflow," *Turbulent Shear Flows II*, edited by L. J. S. Bradbury, F. Durst, B. E. Launder, F. W. Schmidt, and J. H. Whitelaw, Springer-Verlag, Berlin, 1980, pp. 233–245.

[9]Holdeman, J. D., and Srinivasan, R., "On Modeling Dilution Jet Flowfield," AIAA Paper 84-1379, June 1984.

[10]Sherif, S. A., and Pletcher, R. H., "Measurements of the Thermal Characteristics of Heated Turbulent Jets in Crossflow," *Journal of Heat Transfer*, Vol. 111, No. 4, 1989, pp. 897–903.

[11]Lilley, D. G., "Lateral Jet Injection into Typical Combustor Flowfield," NASA CR-3997, July 1986.

[12]McMurry, C. B., Ong. L. H., and Lilley, D. G., "Two Opposed Lateral Jets Injected into Swirling Crossflow," AIAA Paper 87-0307, January 1987.

[13]So, R. M. C., and Ahmed, S. A., "Helium Jets Discharging Normally into a Swirling Air Flow," *Experiments in Fluids*, Vol. 5, No. 4, 1987, pp. 255–262.

[14]Chao, Y. C., and Ho, W. C., "Numerical Investigation of the Heated and Unheated Lateral Jets Discharging into a Confined Swirling Crossflow in a Tube" *Proceedings of the 25th ASME National Heat Transfer Conference*, Houston, TX, ASME, N.Y., N.Y., 1988.

[15]Ho, W. C., "Numerical Investigations of Mixing Between Lateral Jets and the Confined Swirling Crossflow with Density Difference," Ph.D. Dissertation, Institute of Aeronautics and Astronautics, National Cheng-Kung University, R.O.C., 1988.

[16]Launder, B. E., and Spalding, D. B., "The Numerical Computation of Turbulent Flow," *Computational Methods in Applied Mechanics and Engineering*, Vol. 3, No. 2, 1974, pp. 269–289.

[17]Serag-Eldin, M. A., and Spalding, D. B., "Computations of Three-Dimensional Gas Turbine Combustion Chamber Flows," *Journal of Engineering for Power*, Vol. 101, No. 2, 1970, pp. 326–336.

[18]Van Doormaal, J. P., and Raithby, G. D., "Enhancement of the SIMPLE Method for Predicting Incompressible Fluid Flows," *Numerical Heat Transfer*, Vol. 7, No. 2, 1984, pp. 147–163.

[19]Chao, Y. C., and Ho, W. C., "On the Numerical Effects on the Computation of a Round Jet Discharging into a Swirling or Nonswirling Crossflow," *Journal of the Chinese Society of Mechanical Engineers*, Vol. 10, No. 1, 1989, pp. 1–13.

[20]Andreopoulos, J., and Rodi, W., "Experimental Investigation of Jets in Crossflow," *Journal of Fluid Mechanics*, Vol. 138, January 1984, pp. 93–127.

[21]Wang, C., "The Effects of Curvature on Turbulent Mixing Layers," Ph.D. Dissertation, California Institute of Technology, Pasadena, CA, 1984.

[22]Ahmed, S. A., and So, R. M. C., "Characteristics of Air Jets Discharging Normally into a Swirling Crossflow," *AIAA Journal*, Vol. 25, No. 3, 1987, pp. 429–435.